Tunable nitrogen-doped carbon nanoparticles from tannic acid and urea and their potential for sustainable soots

CHEMNANOMAT

CHEMISTRY OF NANOMATERIALS FOR ENERGY, BIOLOGY AND MORE

www.chemnanomat.org

Accepted Article

Title: Tunable nitrogen-doped carbon nanoparticles from tannic acid and urea and their potential for sustainable soots

Authors: Thomas Berthold, Caudia Ramirez Castro, Martin Winter, Gerhard Hoerpel, Mert Kurttepeli, Sara Bals, Markus Antonietti, and Nina Fechler

To be cited as: *ChemNanoMat* 10.1002/cnma.201700051

Link to VoR: http://dx.doi.org/10.1002/cnma.201700051

A Journal of

ACES Asian Chemical Editorial Society

A sister journal of **Chemistry – An Asian Journal** and **Asian Journal of Organic Chemistry**

WILEY-VCH

10.1002/cnma.201700051

Tunable nitrogen-doped carbon nanoparticles from tannic acid and urea and their potential for sustainable soots

Thomas Berthold [1], Claudia Ramirez Castro [2], Martin Winter [2], Gerhard Hoerpel [2], Mert Kurttepeli [3], Sara Bals [3], Markus Antonietti [1] and Nina Fechler [1*]

[1] Max Planck Institute of Colloids and Interfaces, Department of Colloid Chemistry, Am Mühlenberg 1, 14476 Potsdam, Research Campus Golm

[2] MEET - Münster Electrochemical Energy Technology, Corrensstraße 46, 48149 Münster

[3] Electron Microscopy for Materials Science (EMAT), University of Antwerp, Groenenborgerlaan 171, B-2020 Antwerp, Belgium

Keywords: Tannic acid, N-doped carbon, Carbon nanospheres, Sustainable soot synthesis, Li-batteries

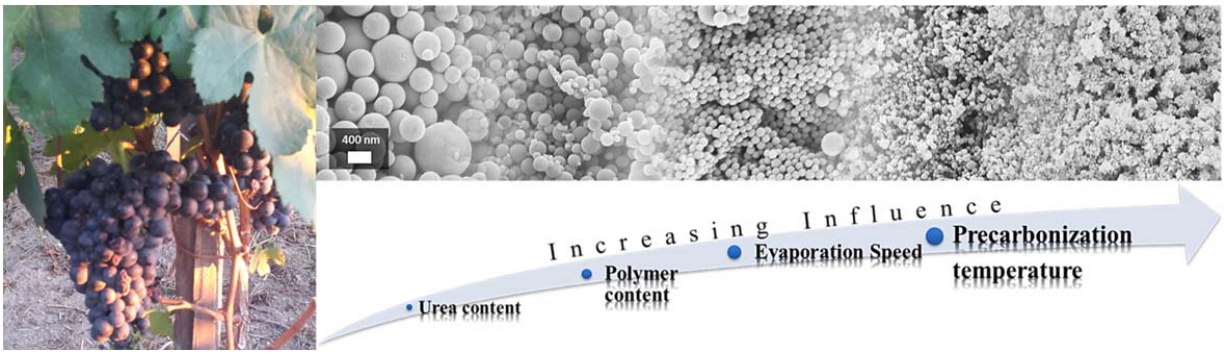

10.1002/cnma.201700051

Abstract

Nano-sized nitrogen-doped carbon spheres are synthesized from two cheap, readily available and sustainable precursors: tannic acid and urea. In combination with a polymer structuring agent, nitrogen content, sphere size and the surface (up to 400 $m^2 g^{-1}$) can be conveniently tuned by the precursor ratio, temperature and structuring agent content. Because the chosen precursors allow simple oven synthesis and avoid harsh conditions, this carbon nanosphere platform offers a more sustainable alternative to classical soots, e.g. as printing pigments or conduction soots. The carbon spheres are demonstrated to be a promising as conductive carbon additive in anode materials for lithium ion batteries.

Introduction

Carbon nanomaterials are one of the classical key-components in many technologies such as batteries, in inks, or supports for catalysts.[1] This is based on the special combination of properties, i.e. high surface area, electric conductivity, high chemical and mechanical stability, and lightweight constitution.[2] For practical electrochemical applications, appropriate surface functionality, wettability, electron and mass transport towards and from the surface, and finally texture are crucial factors.[3] For the latter, especially expanded structured aggregates of primary carbon nanospheres can provide such properties.[4]

Traditionally, such commercial carbons are often produced under rather non- sustainable conditions, e.g. by incomplete combustion of methane or petroleum in a high temperature flame, usually above 1200 °C. These are admittedly harsh, energy consuming, an certainly non-green conditions which are, however, still applied in on largest production scales as the demand for such conductive soots is ever-increasing (annual soot demand in 2014: 11.5 Mt, with the ongoing electrification of vehicles and devices making this number foreseeable explode.[5,6] A more energy, atom efficient and also controllable synthesis, which scales with the demand for current and future energy supply, is thereby eagerly wanted, if it is not an important cost factor. Also for those reasons, alternative preparation techniques for nanocarbons have become the focus of research during the last years.[7] For example, the hydrothermal carbonization (HTC) processes allow the synthesis of micron-sized carbon particles with diameters ranging from 500 nm to 10 µm.[8] Here, glucose as a typical precursor is first converted into carbonaceous particles at low

temperatures and under autogenetic pressure. In a second step, heating to elevated temperatures further converts these particles into the respective carbon.[8] Smaller HTC carbon nanospheres could be synthesized by the addition of acid/base-catalysts or stabilizers during the HTC process.[9-11] More recently, porous carbon nanoparticles with diameters of 200 nm were derived by a HTC process with glucose under hypersaline conditions, i.e. the particle formation in the presence of concentrated salt solutions.[12] Unfortunately, control of particle size at the nano-range remained difficult. Another powerful synthesis pathways towards carbon-nanospheres starts with self-assembly processes of resin-materials.[7,13-15] Yet, these methods usually depend on formaldehyde cross-linked resins from phenol,[16] resorcinol [17] or phloroglucinol [18] contradicting the sustainability aspect. Also here, tuning to lower sizes as well as the introduction of structural aggregates are not described.[7,19]

We present here a cheap and scalable synthesis of nanospherical, nitrogen-doped, structured carbons with adjustable functionality and composition from renewable resources, tannic acid and urea, with a polymeric structuring agent. Tannic acid is a natural polyphenol which possesses redox active moieties, serves as antioxidant, is biocompatible and is already extracted in large quantities, e.g. as aside products from wine making.[20-23] During heating, the peripheral structure of tannic acid usually decomposes.[22] As found in the present study, this can be altered by the addition of urea. Furthermore, urea allows for the convenient introduction of structural nitrogen motives into the final material. In order to guide the morphology of this reaction product, *Pluronic* P123 is used as structuring agent, which can effectively stabilize the formation of spherical nanoparticles. The particle size, nitrogen content and porosity can be concomitantly adjusted by the tannic acid/urea content, temperature and structuring agent concentration.

Results

For the synthesis of nitrogen-doped carbon nanoparticles from tannic acid and urea, the solid precursors are mixed in the wanted ratio and dissolved in a small amount of ethanol This mixture can then be dried and stored for later use. In a second step, this tannic acid/urea premix as well as *Pluronic* P123 are dissolved in ethanol/water mixtures which are then poured in a petri dish forming a pale-yellow homogeneous solution (**Figure 1, a, b**).

10.1002/cnma.201700051

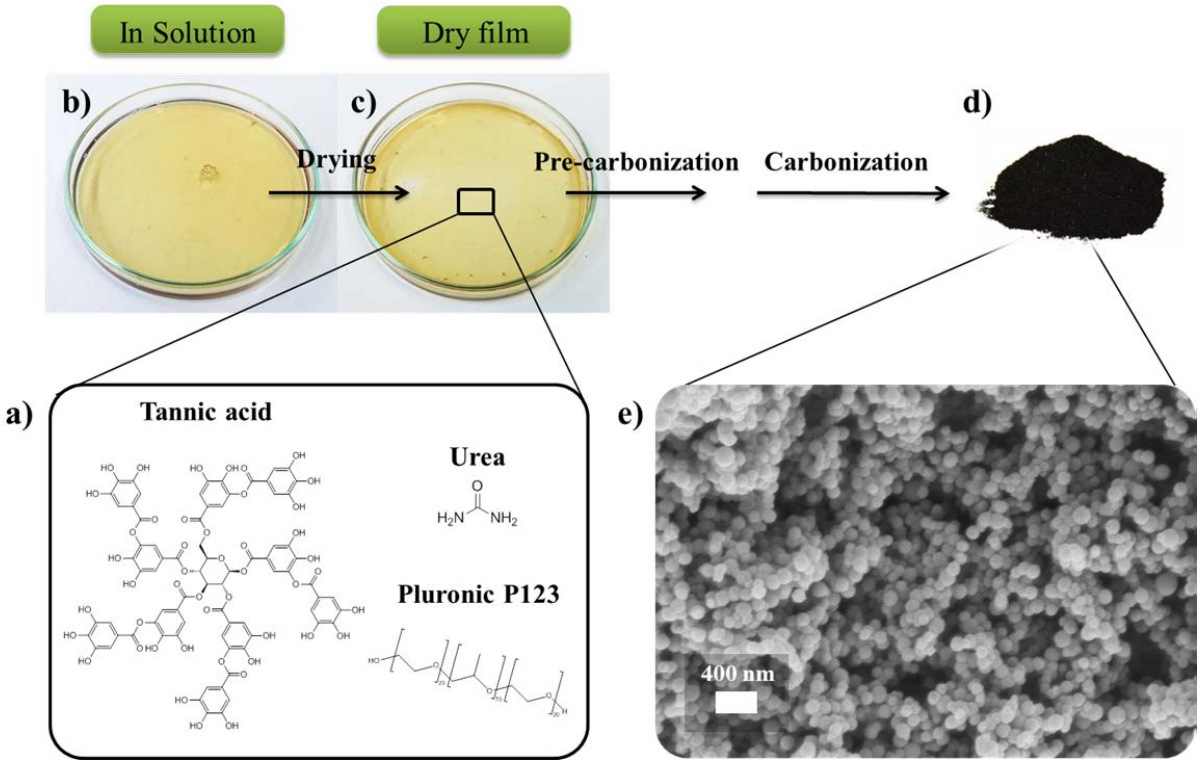

Figure 1 Presentation of the precursors and synthesis steps for nitrogen-doped carbon nanoparticles: a) chemical structure of tannic acid (structural scheme as provided by sigma Aldrich), urea and *Pluronic* P123, b) precursor solution before drying, c) precursor solution after drying at room temperature, d) carbonized powder e) Scanning electron microscopy image of the final carbon nanoparticle aggregates.

The solution is then left drying at different temperatures which results in an orange transparent film (**Figure 1 c**). Further pre-condensation at moderate temperature and heat treatment at elevated temperatures gives the final carbon material (**Figure 1 d**). The scanning electron microscopy (SEM) investigation of the carbon reveals it to be constituted of nanosized spheres (**Figure 1, e**). For comparison, a carbon sample prepared from a mixture of tannic acid and urea without the structuring agent results in an unstructured, non-porous bulk material (**Figure SI-1**).

In order to obtain insights into the precursor system and the structure formation, detailed investigations were performed with and without the structuring agent.

Tannic acid and urea as carbon-precursor system

Polymer-free mixtures of tannic acid and urea (TaUX) were first analyzed by Fourier transform infrared spectroscopy (FTIR). Compared to pure urea the typical FTIR signals of the amine and carbonyl group shifts.[24] In detail, the prepared mixtures TaUX shows up-shifts of the $\nu_s(NH_2)$ and $\nu_{as}(NH_2)$ bands to higher wavenumbers with increasing content of urea **(Figure SI-2)**. This indicates an elongation of the NH-bond and consequently weaker hydrogen bonds involving the amines. Furthermore, the carbonyl group from urea forms energetically more favorable hydrogen bonds with the hydroxyl groups of tannic acid than with the own amine functions.[24] All this speaks for a supramolecular preorganization of the employed monomers, analogous to ref. [25].

Thermogravimetric analysis (TGA) was performed with pure tannic acid, a mixture of tannic acid/urea and a mixture containing *Pluronic* P123 (**Figure SI-3**). Here, tannic acid reveals a 5 wt% mass loss below 220 °C, which can be ascribed to the evaporation of bound water. The following main thermal degradation of tannic acid is observed from 220 °C to 350 °C down to a residual mass of 46 wt%. As reported by Nagarajan et al.[22], the mass loss is mainly related to decarboxylation reactions of the peripheral parts of tannic acid, which results in elimination products such as carbon dioxide and Benzene-1,2,3-triol. Above 350 °C, moderate further decarboxylation of the inner parts of tannic acid [22] proceeds, together with the onset of aromatic condensation reactions. The addition of urea results in a similar TGA profile, however, shifted to lower temperatures, i.e. urea promotes the condensation reactions even of the tannic acid part. (**Figure SI-3**).[22,26,27] The mixture containing *Pluronic* P123 shows an additional thermal decomposition from 330 °C to 370 °C, which is due to the well-known depolymerization (**Figure SI-3**).[17]

Structuring of tannic acid and urea derived carbons

The tannic acid urea precursor system can be structured by several parameters. In order to investigate the influence of synthetic conditions on the resulting carbon-nanostructures, the *Pluronic* P123 amount, urea content, pre-carbonization temperature and drying temperature were systematically varied. For comparison, we choose a moderate final carbonization temperature of 800 °C for all experiments. The samples are denoted following the code given in the experimental part. As example, the sample TaU9_P1_RT was prepared from a tannic acid to urea molar ration of 1 to 9, with the addition of 1 g *Pluronic* P123 and dried at room temperature.

10.1002/cnma.201700051

In general, the X-ray diffraction (XRD) pattern of all carbons reveal typical graphitic domains with broad reflections at 2θ=23.5 ° (002, reflection of disordered stacking of the aromatic carbon layers) and 2θ=44 ° (101, intralayer reflection) (**Figure SI-4** and **SI-5**). Further details of all carbon materials prepared are listed in

Table 1 and will be discussed separately in the following.

Table 1. Combustion elemental analysis (EA), yield and nitrogen sorption data of carbons prepared from tannic acid and urea at varying conditions.

Sample name	EA [wt%]			C/N-ratio	Yield [wt%]	S_{BET} [m²/g]	Sphere diameter (Average) [nm]
	C	H	N				
TaU9_P0.5_RT	83.4	1.8	4.7	17.6	27.7	28	590
TaU9_P1_RT	83.5	1.7	4.5	18.6	31.9	32	460
TaU9_P1.5_RT	86.1	1.7	4.4	19.8	38	44	250
TaU9_P2_RT	85.5	1.7	4.1	21.0	39.7	69	160
Ta_P1.5_O	89.3	1.8	1.2	77.1	37	362	<30
TaU1_P1.5_O	88.3	1.8	2.4	37.2	40.7	295	<30
TaU5_P1.5_O	86.9	1.7	3.3	26.7	40.1	372	<30
TaU9_P1.5_O	85.5	1.6	3.7	23.0	36.4	263	40
TaU13_P1.5_O	86.3	1.7	3.7	23.5	39.4	184	45

The structuring agent content:

Only in the presence of *Pluronic* P123, spherical nanoparticles are obtained from tannic acid and urea, which can then be transformed into the respective carbon nanoparticles by carbonization (**Figure SI-1**). Furthermore, it is found that the amount of *Pluronic* P123 added during the synthesis can be used to control the carbon sphere size in a systematic fashion. Within the first series, the particle sizes gradually range from an average of 590 nm (**Figure 2 a**) down to 160 nm (**Figure 2 d**) in diameter, where a higher content of the structuring agent leads to smaller spheres (**Table 1**, **Figure 2**).

10.1002/cnma.201700051

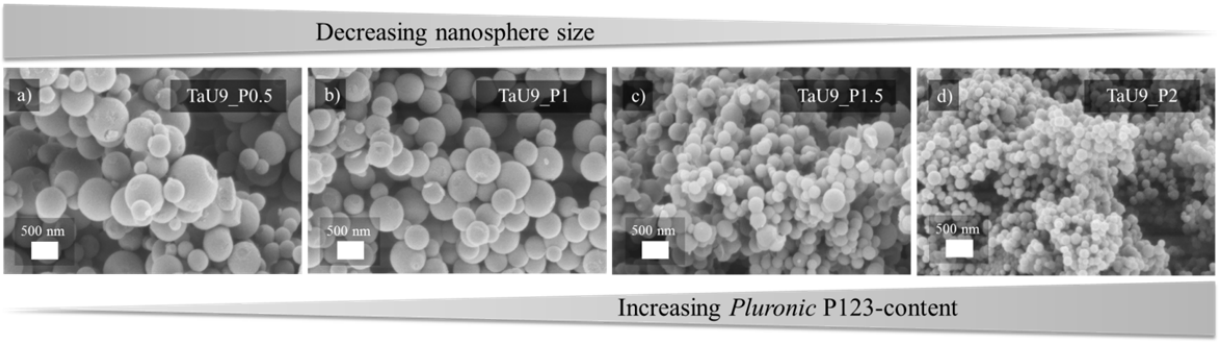

Figure 2 a-d. Influence of *Pluronic* P123 content on the carbon nanosphere size.

The evolution of the spherical morphology in the presence of the structuring agent is ascribed to a microphase demixing between the solvent, structuring agent and material during the drying process, similar to the evaporation-induced self-asembly (EISA). The formation of smaller particles with increasing *Pluronic* content is attributed to the fact that higher amounts of structuring agent can stabilize more surface area in the continuous phase.

Further heat-treatment at elevated temperatures allows for the conversion of the structure into the respective nitrogen-doped carbon nanoparticles. The decreasing nitrogen content and increasing yield with higher amounts of *Pluronic* P123 point to the partial incorporation of the structuring agent into the final carbon during the carbonization process (**Table 1**). This is to be expected as both components consist of organic materials, which can partially react with each other.

Under these conditions, nitrogen sorption analysis of the carbon-nanospheres show medium-range BET-surface areas (28 to 69 m²/g) with a trend to increasing values with increasing *Pluronic* P123 content. This indicates the formation of massive, non-microporous primary particles which, however, reveal accessible interstitial space and outer surface area. (**Table 1**, **Figure SI-6**). Primary carbon particles of about 100 nm diameter are expected to have an outer surface area of ca. 30 m^2/g, that is the specific surface area can be nicely described by a massive sphere model, only.

This is further supported by high angle annular dark field scanning transmission electron microscopy (HAADF-STEM) imaging in combination with energy dispersive X-ray (EDX) spectroscopy and electron tomography which is representatively shown for the sample TaU9_P1_RT (**Figure 3**). The HAADF-STEM image indicates that the nanospheres do not contain pores, neither at their surface, nor in the interior **(Figure 3 a, b**). With regard to the elemental composition, EDX elemental mapping of TaU9_P1_RT reveals a homogeneous

10.1002/cnma.201700051

elemental constitution of carbon and nitrogen (**Figure 3 c, d**). From the 3D visualization of the tomographic reconstruction (**Figure 3 e**) and a slice taken through the reconstruction (**Figure 3 f**), the nonporous nature of the nanospheres is confirmed. An animated version of the 3D reconstruction is provided in the electronic Supporting Information.

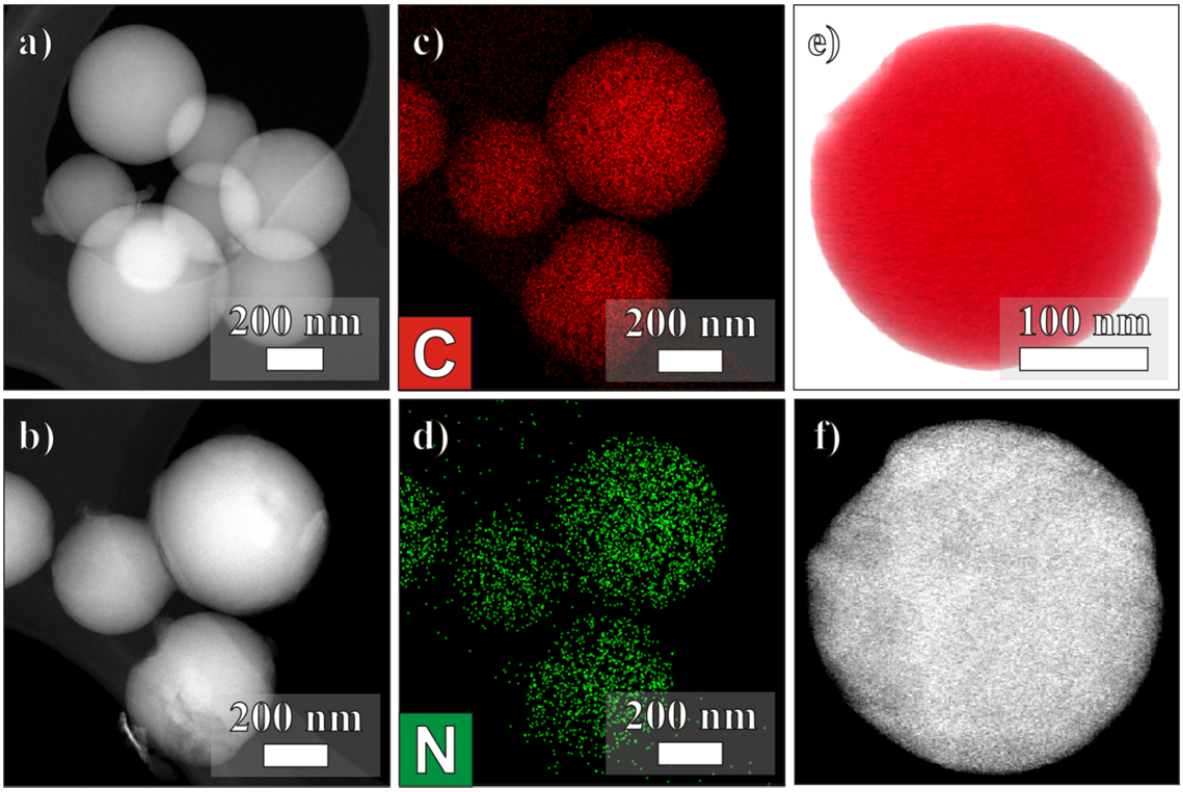

Figure 3 HAADF-STEM, EDX and electron tomography investigations of TaU9_P1_RT: a) HAADF-STEM image showing that the sample consists of nanospheres as described above, b) HAADF-STEM image, c) Carbon and d) Nitrogen EDX elemental maps of the same region, e) 3D visualization of the reconstruction following electron tomography and f) slice through the 3D reconstruction showing the inner structure of the nanosphere.

The pre-carbonization process

As further parameter, the pre-carbonization temperature has a crucial impact on the surface area, particle size, elemental composition and morphology of the final carbon.

On the one hand, higher temperatures result in smaller primary particles (**Table 1**, **SI-2** and **SI-3**; **Figure SI-7, SI-8**). On the other hand, the films turn from transparent orange into brown opaque

10.1002/cnma.201700051

(samples indicated with "O") (**Figure 4**), As "opaque" can be usually related to larger particles, we have to state that obviously secondary aggregation and structure formation takes place at those temperatures.

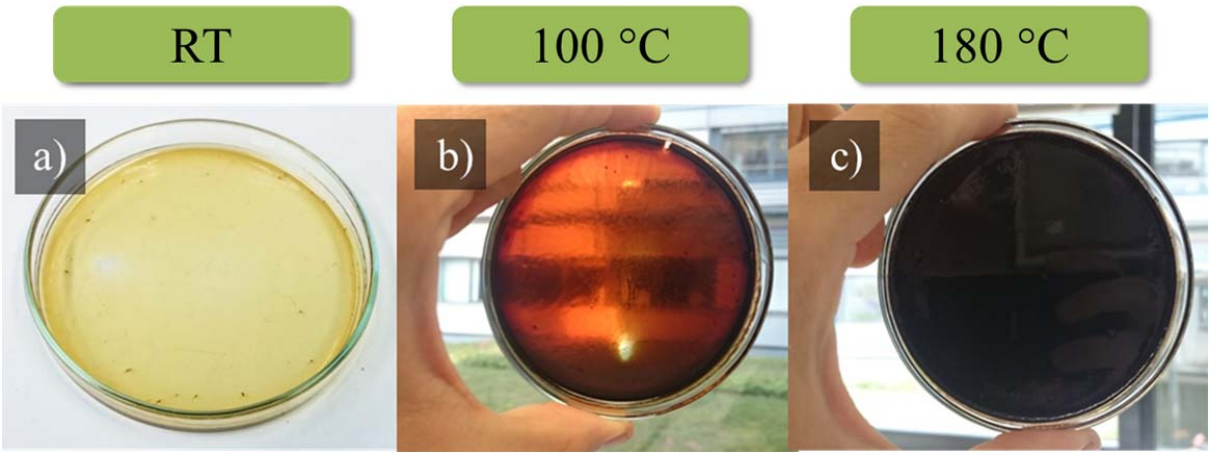

Figure 4 Photographs of precursor films prepared from tannic acid, urea and *Pluronic* at different temperatures exemplarily shown for the mixture TaU9_P1.5: a) dried at room temperature, b) pre-carbonization at 100 °C and c) pre-carbonization at 180 °C.

The color change already indicates the formation of aromatic intermediates from tannic acid and urea already at 100 °C, that is the cross-reaction sets in. At 180 °C the reaction leads to a brown – black material, i.e. aromatic condensation has taken place to allow extended electron delocalization.

The fact that the primary nanospheres are smaller with increasing temperature (**Figure 5; Table 1** and **SI-3**) we attribute to a classical heterophase polymerization effect, the competition of two processes, polycondensation and particle fixation on the one hand a demixing and Ostwald ripening due to interface energy on the other. Higher temperatures simply allow immobilizing the primary particles at an earlier state, and colloidal instability then only leads to the formation of secondary, structures aggregates. This is in fact very similar to the formation of soots in the gas phase, however here in a liquid medium.

Consequently the carbons prepared at higher pre-condensation temperatures reveal much higher surfaces due to small particles (263 m^2/g versus 44 m^2/g vs., **Table 1** and **SI-3**; **Figure SI-8**).

10.1002/cnma.201700051

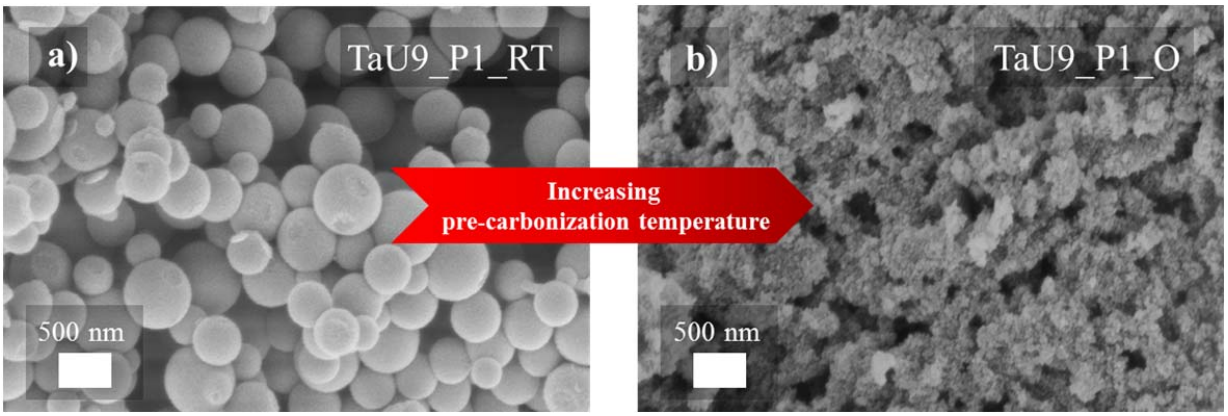

Figure 5 Influence of the pre-carbonization temperature on the carbon nanoparticles.

A surface area of 263 m^2/g pro forma corresponds to a primary particle size of 10 nm, which nicely goes with the electron microscopy observations. Besides the sphere size, higher pre-carbonization temperatures lead to a slightly decreasing nitrogen content in the final carbon material, at fixed urea concentration (**Table 1**), which we describe to urea decomposition prior to cross-condensation.

The urea content

Increasing urea content in the carbon precursor-mixture allows to increase the nitrogen content in the final material (**Table 1**). This indicates the successful cross-condensation of the precursors without complete decomposition or homo-condensation of urea in early stages of the reaction. As processes are highly parallel and cannot necessarily be judged independently, an economic urea content is to be found with regard to the surface area and functionality (**Figure 6**). The maximal surface area of 372 m^2/g (TaU5_P1.5_O) was observed for a urea/tannic acid molar ratio of 5:1, whereas the nitrogen content still increased up to a molar ratio of 9:1 (TaU9).

10.1002/cnma.201700051

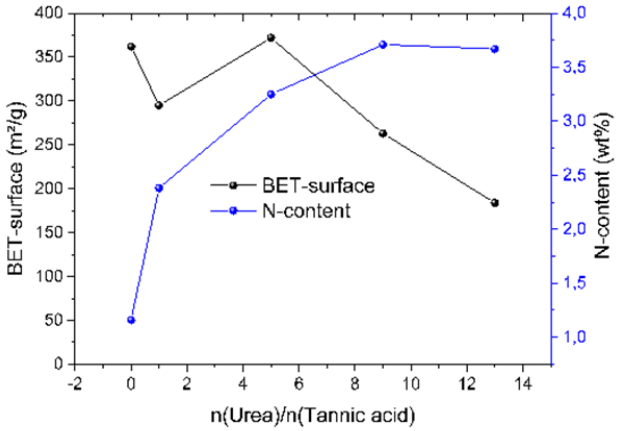

Figure 6 Dependence of BET-surface-area and N-content on the carbon nanoparticles with varied carbon precursor-mixtures.

Ball milling of the carbon materials revealed the expected increase of surface area for samples prepared with low and medium urea content, i.e. the carbons are brittle and can be broken apart. For carbons prepared with higher amounts, this milling effect is only minor, that is the small particles cannot be efficiently fractured, anymore (**Table SI-1**).

Nitrogen-doped carbon nanospheres as conductive additive in the anode of Li-ion batteries

Lithium ion batteries (LIBs) are devices which have to expect focused attention, e.g. due to the electrification of vehicles. Conductive additives are needed to improve their performance at high current cycling regimes to establish sufficient electron pathways. With regard to such applications, the contact theory by Mrozowski and Holm describes the electrical conductivity of a carbon black to be dependent on the particle separation distance, the average size, as well as the composition/functionality on the carbon surface.[28] The herein presented nitrogen-doped carbon nanospheres were designed to possess promising characteristics in this direction and are thus applied as conductive soot for the anode of a Li-ion battery. For this application and the head-to-head comparison with a commercial carbon black (Super C65), one of our nitrogen-doped carbon sample was carbonized at 950 °C (TaUC). It is to be noted that this temperature is much lower than the usual final carbonization temperature of classical conduction soots, i.e. it is usually believed that the quality of electrical conductivity only relates to the degree of graphitization.

This is, however, different for functional, N-doped carbon nanostructures as they develop their properties usually at lower synthesis temperatures.

The elemental composition determined by combustion elemental analysis reveals that the commercial carbon Super C65 is mainly constituted of carbon, whereas the TaUC sample possesses a nitrogen content of 4 wt% (

Table). Assuming complete combustion and the absence of impurities, TaUC contains an additional oxygen content of 4.7 wt%.

Table 2 Elemental analysis from combustion and XPS for TaUC and commercial Super C65.

Sample	Elemental analysis [wt%]				XPS [wt%]		
	C	N	H	O[#]	C	N	O
TaUC	90.4	3.9	1	4.7	95.3	2.8	1.9
Super C65	99.9	-	-	0.1	97.5	-	2.5

[#] Oxygen content calculated as residual mass assuming complete combustion and absence of impurities.

As the conductivity of soots depends on their surface composition, XPS measurements were conducted in order to compare the surface properties of the studied materials. In comparison to the combustion elemental analysis, the nitrogen content of TaUC derived from XPS is slightly lower, which hints to a heteroatom depletion towards the particle outside, known from other systems.[29] For the carbon and oxygen content, both materials reveal similar XPS values with slightly higher amounts for the commercial sample (**Table 2**).

Further evaluation of the XPS data reveals the presence of typical carbon oxygen functionalities (C-O, C=O, COOH) on Super C65 and TaUC, whereas the nitrogen present at the surface of TaUC is attributed to pyridinic and pyrollic moieties (**Figure SI-11**).[30,31] The ratio of the Raman D/G band (I_D/I_G) showes a lower value for TaUC (I_D/I_G = 0.95) than for Super C65 (I_D/I_G = 1.01) (**Figure SI-9**). This can already be explained by the nitrogen incorporation and thus introduction of symmetry defects in the graphene structure, which lead to a broadening of the D-band.[32,33] From the nitrogen sorption measurement of TaUC, a BET-surface area of 167 m²/g (**Figure SI-10**) is calculated, a very typical value for conduction soots with the dense primary particles.

In **Table 3**, the electronic conductivity measurements for the SLP30 (a standard active material composition for LiBs) composite electrodes with TaUC and super C65 as conductive additives are summarized. For both electrodes the electronic conductivity is about 0.8 Scm^{-1} with a slightly higher value for the commercial conductive additive. With regard to the high carbonization temperatures of the commercial conductive additives in the range of 1200 °C, as compared to 950 °C of the nitrogen-doped carbon, this is plausible. In previous works it has been reported that the nitrogen atoms in N-doped carbons act as electron donors and enhance the conductivity of carbonaceous materials (n-type doping). [34,35] which obviously compensates to a large extend for the lower carbonization temperature.

Table 1 Electronic conductivity of TaUC and Super C65 of SLP30 composite-electrodes via Novocontrol measurements.

Sample	Conductivity σ ($S \cdot cm^{-1}$)
SLP30 electrode with TaUC	0.08128
SLP30 electrode with Super C65	0.08597

For a comparative performance evaluation in the real battery system, the rate performance of SLP30 composite electrodes made with Super C65 and TaUC, respectively, as conductive additives were measured (**Figure 7**). The discharge capacity for both working electrodes follow the same trend especially at higher c-rates (1 C to 5 C) with a stable discharge capacity through long term cycling (1 C). In fact, both systems behave rather similar. Keeping in mind that the production of TaUC is more sustainable, performed in a liquid process with much lower energy use and higher atom efficiency and is potentially much cheaper, i.e. is the "green chemistry" product, this is a remarkable result. This even contributes to the economic base and the sustainability of the complete LiB battery (about 10 % of the active material are conduction soots). The results presented herein reveal indeed the TaUC carbon to be highly promising as conductive additive in electrodes even reaching a comparable performance to Super C65, the state of the art conductive additive. This is attributed to the advantageous morphology of extended aggregated nanospheres of the TaUC carbons which allows for the formation of

10.1002/cnma.201700051

interconnected conduction pathways that efficiently percolate the composite electrode even at low soot content.

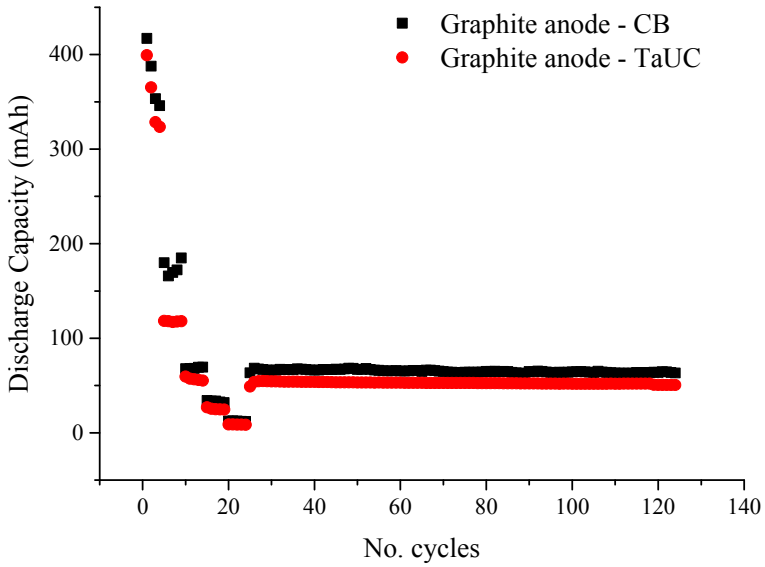

Figure 7 Rate performance of SLP30 composite electrodes prepared with TaUC (red) and Super C65 (black) as conductive additives.

Conclusion

In conclusion, the scalable synthesis of tunable nitrogen-doped carbon nanosphere aggregates from the economic and renewable precursors tannic acid and urea is presented. Carbon properties important with respect to applications such as the nitrogen content, particle sizes and thus surface area, as well as aggregation state could be easily adjusted by varying the precursor ratio, structuring agent content, and synthesis temperature of both polycondensation and carbonization step..

The nitrogen-doped carbon nanospheres were exemplarily applied as conductive soot in the anode of a standard Li-ion-battery set-up. The material revealed a comparable performance to a commercial state of the art carbon black which makes the tannin nanocarbons a both cost effective and more sustainable alternative.

10.1002/cnma.201700051

Acknowledgements

S. B. is grateful for funding by the European Research Council (ERC starting grant #335078-COLOURATOMS).

Experimental

Materials

Tannic acid (M_n = 1702 g/mol; declaration by aldrich), urea, *Pluronic* P-123 and ethanol were purchased from Sigma Aldrich and were used without further purification.

For the electrochemical measurements electrode composites were prepared using SLP30 (Imerys Graphite & Carbon, Bodio, Switzerland) as active material, Super C65 (Imerys Graphite & Carbon) as conductive additive and CMC (Walocel CRT 2000PPA 12, Dow Wollf Celluosics®) and SBR (Lipaton SB 5521, Polymer Latex GmbH) as binders.

Preparation of the Samples and Carbon-nanosphers

*Mixtures of tannic acid and urea (**TaU**X)*

Different ratios of solid tannic acid and urea were mixed. The mixture was dissolved in a small amount of ethanol and dried in air. Afterwards, the air dried product was further dried in a vacuum oven at 60 °C for one day and purely analyzed by FTIR.

*Preparation of the carbon-nanospheres (**TaU**X_**P**Y_Z)*

In a typical synthesis of the carbons, 1 g of a tannic acid/urea mixture and the respective amount of *Pluronic* P123 (Summary of all samples in **Table 4**) were dissolved in a mixture of 18 mL ethanol and 1 mL deionized water. Afterwards, the mixture was poured in a petri dish and dried at 25 °C (denoted as TaU**X**_P**Y**_**RT**) or 120 °C (TaU**X**_P**Y**_**O**), respectively, whereby **X** refers to the molar ratio of urea to tannic acid and **Y** refers to the mass ratio of the *Pluronic* P123 to the total mass of the carbon precursor-mixture. Further, TaUX_PY_**RT** was pre-carbonized at 100 °C for 12 h in an air-oven, whereas TaUX_PY_**O** was pre-carbonized at 180 °C with a reduced reaction time of 2 h (to reduce the effects of oxidation). The resulting black film was placed in ceramic crucibles and heated to 800 °C with a heating ramp of 2.5 °C/min under nitrogen. After holding the target temperature for 1 h the samples were allowed to cool down to room temperature and grinded in a mortar. To check the interconnectivity of the small carbon-nanospheres (sphere diameters below 100 nm), the samples dried at 120 °C were further ball milled and investigated by physisorption before and after ball milling.

10.1002/cnma.201700051

Table 4. Summary of the mixtures and preparation conditions of all samples in this publication.

Sample name	**Mixture of … [mg]**			**Drying temperature** [°C]	**Pre-carbonization …**		**Carbonization temperature** [°C]
	Tannic acid	Urea	*Pluronic* P123		Temperature [°C]	Time [h]	
TaU9_P0_RT	749	251	0	RT	100	12	800
TaU9_P0.5_RT	749	251	500	RT	100	12	800
TaU9_P1_RT	749	251	1000	RT	100	12	800
TaU9_P1.5_RT	749	251	1500	RT	100	12	800
TaU9_P2_RT	749	251	2000	RT	100	12	800
Ta_P1.5_O	1000	0	1500	120	180	2	800
TaU1_P1.5_O	965	35	1500	120	180	2	800
TaU5_P1.5_O	850	170	1500	120	180	2	800
TaU9_P1.5_O	749	251	1500	120	180	2	800
TaU13_P1.5_O	685	315	1500	120	180	2	800
TaUC	749	251	1500	120	180	2	950

For the comparison of the carbon nanospheres and a commercial carbon black, the sample TaUC was prepared with a 9:1 molar ratio of urea to tannic acid, dried at 120 °C, pre-carbonized at 180 °C and carbonized at 950 °C.

Characterization

FTIR was conducted with a Varian 600 FTIR spectrometer.

TGA was measured with a Perkin-Elmer STA 6000 under Nitrogen using a heating rate of 2.5 K/min to mimic the conditions during the carbonization.

Nitrogen sorption measurements were accomplished with N_2 at 77 K after degassing the samples at 150 °C under vacuum for 20 hours using a Quantachrome Quadrasorb SI porosimeter. The apparent surface area was calculated by applying the Brunauer-Emmett-Teller (BET) model to the isotherm data points of the adsorption branch in the relative pressure range $p/p_0 < 0.3$.

WAXS-patterns were measured with a Bruker D8 Advance instrument using Cu-Kα-radiation.

SEM images were obtained on a LEO 1550-Gemini instrument after sputtering with a 20/80 wt% platinum/gold alloy. The obtained images were analyzed by Image J to evaluate the obtained sphere diameters.

Transmission electron microscopy (TEM) specimens were prepared by suspending the powder in ethanol. A drop of this suspension was deposited on a carbon coated TEM grid. High-angle annular dark field scanning TEM (HAADF-STEM) images and energy-dispersive X-ray elemental maps were collected using an aberration corrected cubed FEI Titan operated at 200 kV, equipped with a Super-X detector for EDX analysis.

Combustion elemental analysis was accomplished using a Vario Micro device.

The surface chemistry of the samples was investigated with an AXIS ULTRA HSA Kratos using an Al Kα monochromatic beam (1486.7 eV). XPS survey spectra were recorded with a pass energy of 120 eV. For the measurement, the sample powders were dispersed onto adherent carbon film. The data were collected at room temperature with an operating pressure below 10^{-9} Torr. Data analysis was performed with the software Casa XPS-Kratos, where every spectrum was corrected according to C 1s at 284.5 eV (graphite like carbon).

Raman measurements were accomplished on a Horiba LabRam HR Evolution Raman microscope with a green YAG-laser (532 nm, 20 mW). The dispersive element was a grating with 400 g/mm and the objective an Olympus MPLN50x (50x magnification). The analysis was done in the range of 600-3000 cm^{-1} with an acquisition time of 3 x 40 s with the powder samples mounted on glass slides.

Electrochemical analysis

Composite electrodes were prepared by mixing the active material (SLP 30), conductive additive (Super C65 or TaUC) and the binders (CMC and SBR) in a weight ratio of 92:5:2:1 in aqueous media. The slurry was casted on a Cu foil with a doctor blade and dried at 60 °C overnight. The electrode area was 1.13 cm^2 with a mass loading of around 13 mg/cm^2 and a thickness of 120 µm.

The electronic conductivity of the electrodes was determined by impedance spectroscopy using an Alpha-A Modular Measurement System Novocontrol GmbH, in a frequency range of 10 MHz to 0.1 Hz.

10.1002/cnma.201700051

The galvanostatic tests were carried out in a Maccor 4300 Battery test system with a three-electrode Swagelock® type cell. In this cell configuration, lithium metal (Rockwood Lithium) was used as counter and reference electrode with a non-woven polypropylene separator (Freudenberg FS2190) and LiPF6 1 M in ethylene carbonate/dimethyl carbonate (LP30 Selectilyte™ BASF) as electrolyte. The galvanostatic test was carried out in a potential window between 1.5 to 0.02 V *vs* Li/Li^+. Two formation cycles were done at 0.1 C and subsequently, the C-rate tests were performed between 0.2 C to 5 C within an additional constant current cycling at 1 C during 100 cycles.

References

1. Choi, N.-S. *et al.* Lithiumbatterien und elektrische Doppelschichtkondensatoren: aktuelle Herausforderungen. *Angew. Chemie* **124,** 10134–10166 (2012).
2. Gogotsi, Y. Not just graphene: The wonderful world of carbon and related nanomaterials. *MRS Bull.* **40,** 1110–1121 (2015).
3. Pampel, J. & Fellinger, T.-P. Opening of Bottleneck Pores for the Improvement of Nitrogen Doped Carbon Electrocatalysts. *Adv. Energy Mater.* n/a–n/a (2016). doi:10.1002/aenm.201502389
4. Presser, V., Dennison, C. R., Campos, J. & Knehr, K. W. The Electrochemical Flow Capacitor : A New Concept for Rapid Energy Storage and Recovery. 895–902 (2012). doi:10.1002/aenm.201100768
5. Donnet, J.-B. Fifty years of research and progress on carbon black. *Carbon N. Y.* **32,** 1305–1310 (1994).
6. Goenka, S. *Phillips Carbon Black Limited; Annual Report*. (2014).
7. Zhang, P., Qiao, Z.-A. & Dai, S. Recent advances in carbon nanospheres: synthetic routes and applications. *Chem. Commun.* **51,** 9246–9256 (2015).
8. Titirici, M.-M. & Antonietti, M. Chemistry and materials options of sustainable carbon materials made by hydrothermal carbonization. *Chem. Soc. Rev.* **39,** 103–116 (2010).
9. Fellinger, T. P., White, R. J., Titirici, M. M. & Antonietti, M. Borax-mediated formation of carbon aerogels from glucose. *Adv. Funct. Mater.* **22,** 3254–3260 (2012).
10. Baccile, N., Antonietti, M. & Titirici, M. M. One-step hydrothermal synthesis of nitrogen-doped nanocarbons: Albumine directing the carbonization of glucose. *ChemSusChem* **3,** 246–253 (2010).
11. Zhang, P. *et al.* Improving hydrothermal carbonization by using poly(ionic liquid)s. *Angew. Chemie - Int. Ed.* **52,** 6028–6032 (2013).
12. Fechler, N., Wohlgemuth, S.-A., Jäker, P. & Antonietti, M. Salt and sugar: direct synthesis of high surface area carbon materials at low temperatures via hydrothermal carbonization of glucose under hypersaline conditions. *J. Mater. Chem. A* **1,** 9418 (2013).
13. Fang, Y. *et al.* A low-concentration hydrothermal synthesis of biocompatible ordered mesoporous carbon nanospheres with tunable and uniform size. *Angew. Chemie - Int. Ed.* **49,** 7987–7991 (2010).
14. Liu, J. *et al.* A facile soft-template synthesis of mesoporous polymeric and carbonaceous nanospheres. *Nat. Commun.* **4,** 1–7 (2013).
15. Song, J. C., Lu, Z. Y. & Sun, Z. Y. A facile method of synthesizing uniform resin colloidal and microporous carbon spheres with high nitrogen content. *J Colloid Interface Sci* **431,** 132–138 (2014).
16. Meng, Y. *et al.* A Family of Highly Ordered Mesoporous Polymer Resin and Carbon Structures from Organic - Organic Self-Assembly. 4447–4464 (2006).
17. Liang, C., Hong, K., Guiochon, G. a., Mays, J. W. & Dai, S. Synthesis of a Large-Scale Highly Ordered Porous Carbon Film by Self-Assembly of Block Copolymers. *Angew.*

Chemie **116,** 5909–5913 (2004).

18. Liang, C. & Dai, S. Synthesis of mesoporous carbon materials via enhanced hydrogen-bonding interaction. *J. Am. Chem. Soc.* **128,** 5316–7 (2006).
19. Ma, T.-Y., Liu, L. & Yuan, Z.-Y. Direct synthesis of ordered mesoporous carbons. *Chem. Soc. Rev.* **42,** 3977–4003 (2013).
20. Sacchi, K. L., Bisson, L. F. & Adams, D. O. A review of the effect of winemaking techniques on phenolic extraction in red wines. *Am. J. Enol. Vitic.* **56,** 197–206 (2005).
21. Graham, H. N. Green tea composition, consumption, and polyphenol chemistry. *Prev. Med. (Baltim).* **21,** 334–350 (1992).
22. Xia, Z. *et al.* Unraveling the mechanism of thermal and thermo-oxidative degradation of tannic acid. *Thermochim. Acta* **605,** 77–85 (2015).
23. Reitas, F. Interaction of Different Polyphenols with Bovine Serum Albumin (BSA) and Human Salivary r -Amylase (HSA) by Fluorescence Quenching. 6726–6735 (2007).
24. Keuleers, R., Desseyn, H. O., Rousseau, B. & Van Alsenoy, C. Vibrational Analysis of Urea. *J. Phys. Chem. A* **103,** 4621–4630 (1999).
25. Fechler, N. *et al.* Eutectic Syntheses of Graphitic Carbon with High Pyrazinic Nitrogen Content. *Adv. Mater.* **28,** 1287–1294 (2016).
26. Stradella, L. & Argentero, M. A study of the thermal decomposition of urea, of related compounds and thiourea using DSC and TG-EGA. *Thermochim. Acta* **219,** 315–323 (1993).
27. Schaber, P. M. *et al.* Thermal decomposition (pyrolysis) of urea in an open reaction vessel. *Thermochim. Acta* **424,** 131–142 (2004).
28. Sánchez-González, J., Macías-García, A., Alexandre-Franco, M. F. & Gómez-Serrano, V. Electrical conductivity of carbon blacks under compression. *Carbon N. Y.* **43,** 741–747 (2005).
29. Xiao, B. *et al.* Reactions of Nitrogen and Oxygen Surface Groups in Nanoporous Carbons under Inert and Reducing. *Langmuir* **37,** 3400–3409 (2005).
30. Puziy, A. M., Poddubnaya, O. I., Socha, R. P., Gurgul, J. & Wisniewski, M. XPS and NMR studies of phosphoric acid activated carbons. *Carbon N. Y.* **46,** 2113–2123 (2008).
31. Wang, Y., Shao, Y., Matson, D. W., Li, J. & Lin, Y. Nitrogen-Doped Graphene and Its Biosensing. *ACS Nano* **4,** 1790–1798 (2010).
32. Bulusheva, L. G. *et al.* Effect of nitrogen doping on Raman spectra of multi-walled carbon nanotubes. *Phys. Status Solidi Basic Res.* **245,** 1971–1974 (2008).
33. Liu, J., Webster, S. & Carroll, D. L. Temperature and flow rate of NH3 effects on nitrogen content and doping environments of carbon nanotubes grown by injection CVD method. *J. Phys. Chem. B* **109,** 15769–15774 (2005).
34. Ismagilov, Z. R. *et al.* Structure and electrical conductivity of nitrogen-doped carbon nanofibers. *Carbon N. Y.* **47,** 1922–1929 (2009).
35. Wiggins-Camacho, J. D. & Stevenson, K. J. Effect of Nitrogen Concentration on Capacitance, Density of States, Electronic Conductivity, and Morphology of N-Doped Carbon Nanotube Electrodes. *J. Phys. Chem. C* **113,** 19082–19090 (2009).